J. Plasma Physics (1998), *vol.* 60, *part* 2, *pp.* 215–228. Printed in the United Kingdom
© 1998 Cambridge University Press

Spatial structure of a nonlinear wave of stratification

M. ROTTMANN and K. H. SPATSCHEK
Institut für Theoretische Physik I, Heinrich–Heine–Universität Düsseldorf,
D–40225 Düsseldorf, Germany

(Received 11 January 1997 and in revised form 12 January 1998)

The positive column of a gas discharge is investigated in the subcritical regime when no self-excited nonlinear ionization wave exists. We derive a model equation for the so-called wave of stratification, which is an externally excited envelope wave. The main point of this work is that, in contrast to previous papers, we take into account the radial structure of the homogeneous column. The mathematical description of the wave of stratification in the form of a complex Ginzburg–Landau equation follows by a systematic reductive perturbation method. The coefficients in the Ginzburg–Landau equation are first calculated in general and are then evaluated explicitly for a low-pressure argon discharge. The results are compared with those obtained from a frequently used simpler model that neglects any radial structure. Finally, the dynamics of the nonlinear wave of stratification is demonstrated via numerical simulations.

1. Introduction

Ionization waves in gas discharges have been well-known phenomena since the last century (Pekarek 1968; Nedospasov 1968; Oleson and Cooper 1968; Landa *et al.* 1980). The attractive optical properties of stratified bright and dark zones in the positive column of a gas discharge can easily be observed, for example, in time-resolved photographs. The frequencies of the ionization waves lie in the range of 1–100 kHz, and their wavelengths are usually only slightly larger than the diameter of the discharge tube.

It is generally believed that the origin of the striated column is a wave phenomenon. The relative change in the electron concentration is responsible for the varying luminosity. Its distribution in space is mainly determined by particle diffusion to the tube walls and the creation of new charge carriers in the volume by collisional ionization. In this respect, the dependence of the ionization rate on the electron temperature is very important. We shall come back to this point later. For simplified models, one can assume that the electron energy transport due to heat conduction is approximately balanced by the Joule heating. Then, the mathematical description of the system is closed when, for a constant current in the gas discharge, the electric field is determined through the pressure force balance. The resulting anomalously dispersive waves (moving striations) have group velocities directed from the cathode to the anode, and phase velocities in the opposite direction. Standing striations, showing a constant (in time) spatial stratification of the plasma column, are special types of that wave phenomenon. They have zero

https://doi.org/10.1017/S0022377898006801 Published online by Cambridge University Press

frequencies but non-zero wavenumbers. Moving striations are usually observed in noble gases (e.g. neon, argon and helium), whereas standing striations occur preferentially in molecular gases (e.g. hydrogen and nitrogen). As has been discussed by Landa (1996), this difference is caused by the different values of the strengths of the electric fields in noble and molecular gases.

Another aspect is important. The ionization wave can be either stable or unstable. In the parameter space given by the (scaled) neutral-particle pressure p_0R and the (scaled) discharge current I/R (where R is the radius of the discharge tube) a curve exists that separates the homogeneous column from the self-excited striated state. In the homogeneous region near the transition curve it is possible to excite (externally) finite-amplitude ionization wave packets with a finite extent in the axial direction. The excitation procedure makes use, for example, of a burst pulse at an additional electrode inside or outside the discharge tube (Yoshimoto and Yamashita 1967). The resulting (not self-generated) wavepackets are called waves of stratification. It can be expected that singular bursts of stable ionization wave packets can also occur in natural low-temperature plasmas.

From the basic mechanism of ionization waves, it is obvious that losses originating from diffusion to the tube wall are important. Thus any reliable theory of the wave of stratification has to take into account radial variations besides the obvious space dependence in the direction of propagation. The main purpose of the present work is to develop a nonlinear theory of the wave of stratification which consistently takes into account the radial structure.

Let us briefly mention some important previous work. The linear, spatially one-dimensional theory (which describes many characteristic features of ionization waves) was developed by Wojaczek (1962). One of the first one-dimensional nonlinear models describing the wave of stratification was presented by Bekki (1981). A linear model with radial structure, including a boundary sheet, was given by Twomey and Franklin (1974). A nonlinear model that takes care of the radial effects in detail has so far been missing. Therefore here we generalize Bekki's nonlinear model based on Wojaczek's equations to two dimensions and compare the results with those of the much simpler one-dimensional models.

Before starting with this programme, we would like to mention another (more procedural) aspect that often is not mentioned explicitly in nonlinear wave theory. It concerns the difference between nonlinear wave propagation in stable and weakly (marginally) unstable systems. In the latter, the slaving principle can usually be enforced, i.e. a few unstable modes dominate the dynamics of the whole system. The mathematically correct procedure for such a situation is centre manifold theory. The latter is a clear prescription for determining the dynamical evolution of the amplitude(s) of a (few) unstable mode(s). Since the most unstable mode(s) slave(s) the rest, from the mathematical point of view the system is actually of low dimension (at least as far as rigorous centre manifold theory has been developed). The situation is different in the (weakly) stable situation. Here one usually has a broadband excitation, and many modes take part in the dynamics. Thus one has to take into account a band of modes. The latter may be centred around a certain (e.g. the least damped) wavenumber, but nevertheless a continuum of modes determines the pulse propagation. In other words, the mathematical procedures to determine the propagation of a wave packet in a (weakly) stable system is different from the description of the amplitude dynamics in an unstable system. For the present problems, this means that we can use the so called Newell–Whitehead procedure

https://doi.org/10.1017/S0022377898006801 Published online by Cambridge University Press

for modelling the wave of stratification. The stabilization of self-excited (linearly unstable) ionization waves (using centre manifold theory) is a topic that will be presented in a forthcoming paper.

The paper is organized as follows. In Sect. 2 we present the model equations obtained from the macroscopic (plasma-dynamical) equations. Section 3 deals with the derivation of a complex Ginzburg–Landau equation for the envelope of the wave of stratification. In Sect. 4 we discuss the specific predictions for a low-pressure argon discharge and present numerical simulations.

2. Basic equations

The plasma in the positive column of a low-pressure gas discharge is weakly ionized and consists of neutral atoms, electrons and positive ions. The dynamics of the charged particles is dominated by collisions with neutral particles. In these collisions, free electrons and ions are produced, while the main particle losses are due to diffusion to the walls. In general, the dynamics underlying that scenario is very complex, and requires a detailed investigation of the various kinetic processes. Introducing particle distribution functions f_α for particles of 'species α' (electrons, ions, metastable atoms, etc.), we can formulate Boltzmann equations of the form

$$\hat{D}_\alpha f_\alpha = \sum_\beta J(f_2, f_\beta) + J^*_\alpha, \tag{1}$$

where the operator

$$\hat{D}_\alpha \equiv \partial_t + \mathbf{v} \cdot \boldsymbol{\nabla} + \frac{q_\alpha}{m_\alpha} (\mathbf{E} + \mathbf{v} \times \mathbf{B}) \tag{2}$$

has been introduced, with q_α being the charge and m_α the mass of a particle of species α. A detailed description of the various processes determining the two-particle contributions $J(f_\alpha, f_\beta)$ as well as the many-particle contributions J^*_α can be found, for example, in the book by Mitchner and Kruger (1973). An appropriate consideration of the intermediate steps in the many-particle processes allows simplification to a three-species model (for electrons, ions and neutrals), taking into account step processes only in an effective manner. It turns out that, by such a procedure, although it is not exact, many physical processes in low-temperature plasmas can be incorporated in a satisfactory way. The ionization waves in which we are interested are slow and the length scales (being of the order of the radius of the discharge tube) are large. Thus a macroscopic plasma-dynamic description is appropriate. Of course, the hydrodynamic description is not valid in the whole range of plasma parameters. In particular, in the limit of low pressures and small currents the kinetic properties of the electrons become important.

For the analytical theory, we use the particle continuity and momentum transfer equations for both charge carriers. In addition, the energy balance for electrons is important. The ion energy balance can be dropped, since the cold ions are in thermal equilibrium with the cold background of neutral particles. Inclusion of the electron energy balance is, however, mandatory. The reason is the sensitive dependence of the ionization rate on temperature. Additionally, we assume quasineutrality. In a small region close to the wall the hypothesis of quasineutrality is not justified. Therefore our model only describes the core of the discharge. At the boundary (wall) we take the density to be zero. Furthermore, we assume constant temperatures and a constant parallel electric field across the discharge. The positive column

https://doi.org/10.1017/S0022377898006801 Published online by Cambridge University Press

is expected to have azimuthal symmetry. The same symmetry is imposed on the ionization waves under consideration. This means that the odd radial derivatives vanish on the symmetry axis. A macroscopic description still requires a detailed calculation of the transport and rate coefficients. These coefficients follow by integration from (approximate) solutions of the kinetic equations. For the details of these calculations, we refer to the literature (Shkarofsky *et al.* 1966; Mitchner and Kruger 1973). At the present stage it is sufficient to note that transport theory provides us with the explicit forms of the coefficients. We shall come back to this point when we present the model equations in detail.

Along the tube, the charge carriers drift with constant velocities (in opposite directions to each other, depending on the signs of the charges). The momentum transfer equations can then be simplified by the drift approximation. The electric current in the discharge is mainly carried by the electrons because of the large mobility of the latter in comparison with that of the ions. In the radial direction, the charge carriers drift with the same velocities. Making use of these assumptions, we can combine the continuity equations. Compared with the work of Wojaczek (1962), no effective loss term (i.e. no effective lifetime of charge carriers) has to be introduced, since we keep the radial dynamics. The radial derivatives in the temperature balance can be neglected, since the radial transport is suppressed by ambipolar diffusion. In summary, we end up with the following set of six equations:

$$0 = \nabla_\parallel (n v_{e\parallel}), \tag{3}$$

$$nZ(n, T_e) = \partial_t n + \nabla_\parallel (n v_{i\parallel}) + \nabla_\perp (n v_{a\perp}), \tag{4}$$

$$n v_{e\parallel} = -b_e (n E_\parallel + T_e \nabla_\parallel n + \gamma n \nabla_\parallel T_e), \tag{5}$$

$$v_{i\parallel} = b_i E_\parallel, \tag{6}$$

$$0 = \nabla_\parallel (\zeta n v_{e\parallel} T_e) - \kappa b_e n T_e \nabla_\parallel^2 T_e + n v_{e\parallel} E_\parallel + nH(T_e), \tag{7}$$

$$n v_{a\perp} = -D(\gamma n \nabla_\perp T_e + T_e \nabla_\perp n). \tag{8}$$

Here n represents the charge-carrier density ($n \approx n_e \approx n_i$), $v_{e\parallel}$ and $v_{i\parallel}$ are the respective drift velocities in the axial direction, $v_{a\perp}$ is the ambipolar drift velocity in the radial direction, b_e and b_i are the electron and ion mobilities respectively, D is the ambipolar mobility, which is approximately equal to the ion mobility, T_e is the electron temperature, and $E_\parallel$ is the axial electric field. H is an energy loss per volume and time, and Z is the ionization rate per unit volume. The latter quantities depend on density and temperature. While the dependence of H on n is negligible, the dependence of Z on n is important for the existence of self-excited ionization waves. The real constants ζ, γ and κ describe the transport properties of electrons, i.e. the thermal convection, the thermal diffusion and the heat conduction respectively.

We normalize the density n, the temperature T_e and the electric field $E_\parallel$ by the corresponding values on the symmetry axis of the homogeneous column. In addition, the time is scaled by the ionization rate per unit volume Z on the axis, and the lengths are normalized by the corresponding ratio $T_e/E_\parallel$. The velocities $v_{e\parallel}$ and $v_{i\parallel}$ and the quantities b_i and H can be normalized by the value of b_e on the axis. In the following sections we do not change the notation and use for the non-dimensional quantities the same abbreviations as so far for the dimensional

https://doi.org/10.1017/S0022377898006801 Published online by Cambridge University Press

quantities. To have a concrete application in mind, we present an example and take the following typical values for normalizations: density $\bar{n}_0 = 2.7 \times 10^{12}$ cm^{-3}, time $\bar{t}_0 = 2 \times 10^{-4}$ s, temperature $\bar{T}_0 = 1.3$ eV, electric field strength $\bar{E}_0 = 0.36$ V cm^{-1}, length $\bar{L} = 3.611$ cm, mobility $\bar{b}_0 = 5 \times 10^4$ cm^2 V^{-1} s^{-1} and ionization rate $\bar{Z}_0 = 4985$ s^{-1}, to obtain for the non-dimensional quantities $\gamma = -0.5$, $\zeta = 1$, $\kappa = 1$, $b_i = 0.026$, $D = 0.026$ and $b_e = 1$, $Z(\bar{n}_0, \bar{T}_0) = 1$ and $H(\bar{n}_0, \bar{T}_0) = 1$. The ionization coefficient depends on n and T, and the first Taylor coefficients are $z_n = 0.75$, $z_{nn} = -1$, $z_{nnn} = 0$, $z_T = 8.5$, $z_{TT} = 56$ and $z_{TTT} = 242$. The dependence of H and T (no n dependence) is taken into account via the Taylor coefficients $h_T = 3.5$, $h_{TT} = -5.5$ and $h_{TTT} = 11$. Of course, other plasma parameters can easily be used.

3. Complex envelope equation

3.1. Homogeneous column at zeroth order

At zeroth order, the assumption of a constant radial electron temperature distribution is a good approximation for the homogeneous positive column, at least for moderate discharge currents (Papoular 1965). Therefore the zeroth-order state can be described by a single equation for the (zeroth-order) density $n = n_0$:

$$n_0 Z(n_0) = -D\nabla_\perp^2 n_0. \tag{9}$$

The ionization rate per unit volume $Z(n_0)$ will be approximated by a truncated Taylor series. Then the resulting nonlinear differential equation (9) is solved numerically. The first zero of n_0 should occur at the boundary R, i.e. the effective discharge-tube radius. The resulting density distribution is close to a Bessel function. An exact Bessel profile occurs for a constant ionization frequency. Because of decreasing ionization rates per unit volume with decreasing densities, the exact density profile is widened in comparison with that for a constant ionization rate. To lowest order, all other quantities (except the density) are assumed to be constant across the homogeneous column.

3.2. Linear equations at first order

We use subscript '0' to indicate quantities describing the zeroth-order homogeneous positive column, and subscript '1' for linear deviations. The current density distribution is assumed to be independent of time and to be constant along the discharge. The mobility b_e is assumed not to depend on temperature. Combining the basic equations (3)–(8), anticipating $j = -env_{e\|} = -en_0 v_{e0\|}$, we can reduce the basic equations to a set of three nonlinear equations:

$$0 = nE + \gamma n \nabla_\| T + T\nabla_\| n + \frac{v_{e0\|} n_0}{b_e}, \tag{10}$$

$$0 = \partial_t n + b_i \nabla_\| (nE) - nZ(n,T) - D\nabla_\perp(\gamma n \nabla_\perp T + T\nabla_\perp n), \tag{11}$$

$$0 = \zeta n_0 v_{e0\|} \nabla_\| T - \kappa b_e n T \nabla_\|^2 T + v_{e0\|} n_0 E + nH(T). \tag{12}$$

Next, (10)–(12) are linearized around the homogeneous state. At first order, we obtain

$$0 = (1 + \nabla_\|) n_1 + (\gamma n_0 \nabla_\|) T_1 + (n_0) E_1, \tag{13}$$

https://doi.org/10.1017/S0022377898006801 Published online by Cambridge University Press

$$0 = (\partial_t + b_i\nabla_\parallel - Z - z_n n_0 - D\nabla_\perp^2)n_1 + \{-z_T n_0 - D[\gamma n_0 \nabla_\perp^2 + (\gamma+1)(\nabla_\perp n_0)\nabla_\perp + (\nabla_\perp^2 n_0)]\}T_1 + (b_i n_0 \nabla_\parallel)E_1, \quad (14)$$

$$0 = n_1 + (h_T n_0 - \kappa n_0 \nabla_\parallel^2 - \zeta n_0 \nabla_\parallel)T_1 + (-n_0)E_1, \quad (15)$$

where z_n, z_T and h_T denote the derivatives of Z and H with respect to n and T respectively. We consider harmonic perturbations in the z-direction, i.e. all quantities are proportional to $\exp[i(kz - \omega t)]$. This leads to the radial eigenvalue problem

$$Mn_1 - N\nabla_\perp^2 n_1 + P\nabla_\perp[(\nabla_\perp \ln n_0)n_1] = i\omega n_1. \quad (16)$$

Here

$$M = A + BK, \quad N = D(1+\gamma K), \quad P = DK(1+\gamma),$$

and the coefficients are

$$A = b_i k^2 - Z(n_0) - z_n(n_0)n_0, \quad B = \gamma b_i k^2 - z_T, \quad K = -\frac{2+ik}{h_T + \kappa k^2 - i(\zeta - \gamma)k}.$$

In general (for a non-simplified homogeneous solution n_0), an analytical solution of the eigenvalue problem (16) is not possible. Therefore we have to solve the eigenvalue problem numerically. We use a standard solver for general complex eigenvalue problems from the EISPACK library.

As can be seen from the linear equations, the real part of ω is symmetric and the imaginary part antisymmetric in k. Figure 1 shows the imaginary part of ω (its sign determines growth or damping) belonging to the three least damped modes. We have chosen the parameters such that one mode is marginal while all other modes are damped. The radial structure of the marginal mode is almost the same as the radial dependence of the zeroth-order density n_0; see Fig. 2. It turns out that the eigenfunctions are almost independent of the wavenumber k. This partly justifies the previously used reductions to one spatial coordinate, as will also become clear later from the numerical simulations. The radial structure of ionization waves was measured by Ohe *et al.* (1991). Their results also show the almost-identical forms of the radial profils of the positive column and the ionization wave.

Later we shall also need the solutions of the adjoint eigenvalue problem

$$M^\star f - N^\star \nabla_\perp^2 f - P^\star(\nabla_\perp \ln n_0)\nabla_\perp f = -i\omega^\star f, \quad (17)$$

with the same boundary conditions as before – now of course for f instead of n_1. It is easily proved that

$$f = n_0^{-P^\star/N^\star} n_1^\star \quad (18)$$

satisfies (17) when n_1 satisfies (16).

It should be mentioned that the linear regime has been intensively examined over the last 30 years. The basic linear processes are now understood correctly. It is important that the temperature is introduced as an independent variable. Many features – especially those of noble gases – can be explained, at least qualitatively. For example, the linear analysis explains the fact that the phase velocity and the group velocity have opposite directions. For a better quantitative agreement, Pekarek, Wojaczek and many others determined the characteristic transport coefficients from the microscopic theory of elastic collisions and took the still-undetermined parameters describing the influence of inelastic collisions from experimental results. Other phenomena (e.g. similiarity laws) could be derived under some weak

https://doi.org/10.1017/S0022377898006801 Published online by Cambridge University Press

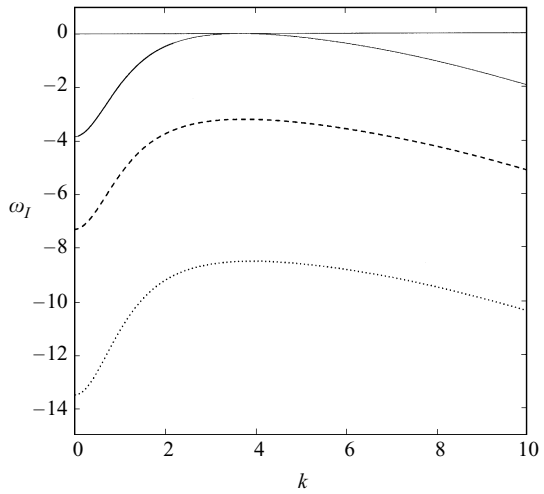


Figure 1. Imaginary part ω_I of the linear frequency ω versus the wavenumber k. Three solutions of the linear dispersion relation, corresponding to the three least-damped modes, are shown.

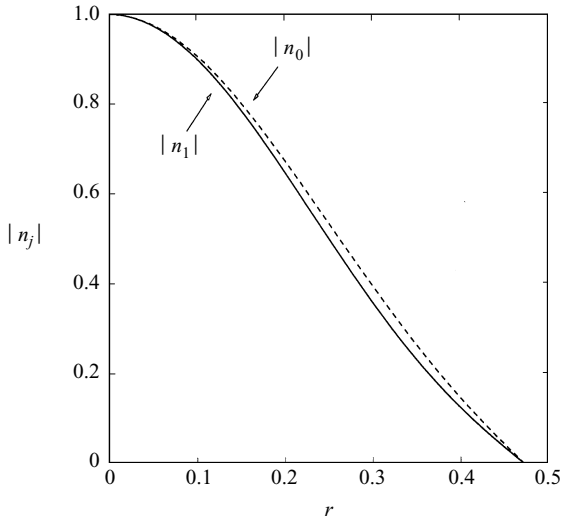


Figure 2. Normalized density distributions n_j for $j = 0$ (zorth order) and $j = 1$ (first order) over the radius r. The zeroth order corresponds to the homogeneous positive column, and the first order is the radial structure of the least-damped density perturbation n_1.

assumptions (Pfau *et al.* 1969), and allow understanding of the similarities in discharges of different sizes. This way of analysing linear ionization waves in glow discharges was quite successful, but linear theory cannot explain the whole variety of observations. One aspect is the (nonlinear) amplitude–width relation; its further understanding is the purpose of the present paper.

3.3. Nonlinear equations

When considering wave excitations, the linear approximation is only valid for (infinitely) small amplitudes. Usually, any external excitation mechanism forces finite

https://doi.org/10.1017/S0022377898006801 Published online by Cambridge University Press

amplitudes, and therefore the nonlinear terms in (10)–(12) become important. (Obviously, in an unstable situation the unstable modes grow and naturally leave the region of validity of the linear approximation.) The idea of the present subsection is to find an approximate (but physically reasonable) solution to (10)–(12). The general solution of the initial-value problem is too complicated, and therefore we restrict attention to the weakly nonlinear regime, where we can apply scaling arguments. We assume that the damping is small, and we scale the (non-dimensional) finite amplitudes (order ϵ) in the same way as the (square root of the non-dimensional) damping rate. Applying that procedure, we can reduce (10)–(12) to a much simpler equation. The latter is known as the Ginzburg–Landau equation, and has been studied intensively during the last few decades. Thus, by finding in the weakly nonlinear regime a physically equivalent but mathematically much simpler equation, we can reduce the general model (10)–(12) to a tractable (generic) formulation. The aim of this calculation is to explain the experimentally observed fact that an initially strongly localized perturbation develops into a wave packet that moves to the anode. The ratio of the central wavelength to the width of the wave packet turns out to be of the same order ϵ as the amplitude.

We now derive, by means of the so-called Newell–Whitehead reductive perturbation method (Newell and Whitehead 1969), the nonlinear envelope equation for the wave of stratification. For the applications we shall use the atomic data for noble gases.

Let us write (10)–(12) in the matrix representation

$$T\partial_t U + A(U)\partial_z U + C(U)\partial_{zz} U + B(U) = 0, \tag{19}$$

with vectors

$$B = \begin{pmatrix} nE + \dfrac{v_{e0\|}}{b_e n_0} \\ -nZ(n,T) - D\nabla_\perp(\gamma n \nabla_\perp T + T\nabla_\perp n) \\ v_{e0\|}E + nH(T) \end{pmatrix}, \quad U = \begin{pmatrix} n \\ T \\ E \end{pmatrix}, \tag{20}$$

and matrices

$$T = \begin{pmatrix} 0 & 0 & 0 \\ 1 & 0 & 0 \\ 0 & 0 & 0 \end{pmatrix}, \quad A = \begin{pmatrix} T & \gamma n & 0 \\ b_i E & 0 & b_i n \\ 0 & \zeta v_{e0\|} n_0 & 0 \end{pmatrix}, \tag{21}$$

$$C = \begin{pmatrix} 0 & 0 & 0 \\ 0 & 0 & 0 \\ 0 & -\kappa b_e n T & 0 \end{pmatrix}. \tag{22}$$

The zeroth-order solution, i.e. the homogeneous discharge column, is $U^{(0)} = (n_0, 1, 1)^{\mathrm{t}}$. Let us expand (19) around the critical point. At the latter, exactly one mode is marginally stable. In the following, we shall use the expansion parameter ϵ, having in mind that the amplitude of the wave ($\propto \epsilon$) scales with the square root of the damping, which is given by the deviation from the critical point. We write

$$U = \sum_{\alpha=0}^{\infty} \epsilon^\alpha U^{(\alpha)} = \sum_{l=-\infty}^{\infty} U_l X_l = \sum_{\alpha=0}^{\infty} \sum_{l=-\infty}^{\infty} \epsilon^\alpha U_l^{(\alpha)} X_l. \tag{23}$$

Here the harmonic phases $X_l = \exp[il(kz - \omega t)]$ and the slowly varying amplitudes $U_l^{(\alpha)}$ have been introduced. The idea behind this expansion is as follows. We expect

https://doi.org/10.1017/S0022377898006801 Published online by Cambridge University Press

to find a wave packet with a certain central wave number k and width, which we write in a Fourier representaion. Actually two spatial scales should determine the packet: (i) the wavelength of the central mode and (ii) its width. If the wave envelope is slowly varying (broad envelope), the Fourier representation can be written in the form presented above. Next, we define the new coordinates

$$\xi = \epsilon(z - \lambda t), \quad \tau = \epsilon^2 t. \tag{24}$$

The smallness parameter ϵ corresponds to the ratio of the central wavelength $2\pi/k$ to the width of the wave packet. Inserting (24) and the expansion (23) into (20), a hierarchy of differential equations is obtained. These equations are ordered with respect to the harmonics and the powers in ϵ. The inhomogeneous equations require that solvability conditions be satisfied. The latter are evaluated with the aid of the adjoint solutions $V_1 = (f_n, f_T, f_E)$ of the linear eigenvalue equation. We shall use the standard scalar product for cylindrical symmetry in complex vector spaces,

$$\langle f|g\rangle = \int_0^R dr\, r \left(\sum_{i=1}^{3} f_i^\star g_i\right) dr.$$

With the linear operators

$$W_l = -il\omega T + ilkA^{(0)} - (lk)^2 C^{(0)} + [\nabla B]^{(0)}, \tag{25}$$

where

$$A^{(0)} = A(U^{(0)}), \quad C^{(0)} = C(U^{(0)}), \quad [\nabla B]^{(0)} = \left(\frac{\partial B}{\partial n}, \frac{\partial B}{\partial T}, \frac{\partial B}{\partial E}\right)(U^{(0)}), \tag{26}$$

we obtain equations of the form $W_l U_l^{(\alpha)} = I_l^{(\alpha)}$ for the lth harmonic at order α. Since W_l is invertible for all l except $|l| = 1$, most equations can be solved directly. It is assumed that at first order only $U_1^{(1)}$ does not vanish, whereas all other harmonics are generated at higher order (a broad wave envelope). The first-order calculation yields the linear dispersion relations, and the second-order solvability condition determines the velocity of the moving frame,

$$\lambda = \frac{\partial \omega}{\partial k}, \tag{27}$$

i.e. the group velocity at the central wavenumber. Zeroth and second harmonics arise at second order. At third order, additional contributions to the fundamental mode appear. The linear mode $U_1^{(1)} = R_1\phi$ is now split into two parts, the radial structure $R_1(r)$ (depending on the radial coordinate r) and the slowly varying amplitude ϕ (as a function of ξ and τ). When writing down the set of equations that follows by the above procedure, we are confronted with a huge algebraic problem. Fortunately, we can use methods developed in another field (Hasegawa 1990) to find the solution systematically. Although the present problem is even more complicated than the standard optical soliton problem, one can obtain the necessary expressions step by step. In order to save space and to concentrate on the main physical results, we do not present the mathematical details here. After some lengthy calculations, the solvability condition for the first harmonic at third order yields a complex Ginzburg–Landau equation for ϕ:

$$i\partial_\tau \phi + P_2 \partial_{\xi\xi}\phi + Q|\phi|^2\phi = 0, \tag{28}$$

https://doi.org/10.1017/S0022377898006801 Published online by Cambridge University Press

where P_2 and Q are complex coefficients. P_2 is determined by the group dispersion

$$P_2 = \frac{1}{2}\frac{\partial^2 \omega}{\partial k^2}, \tag{29}$$

and Q originates from the nonlinear coupling of the waves:

$$Q|\phi|^2\phi = \frac{\langle V_1 | Q_1^{(3)} \rangle}{\langle V_1 | - iTR_1 \rangle}. \tag{30}$$

Here $Q_1^{(3)}$ is the nonlinear part in $I_1^{(3)}$, and V_1 is the adjoint eigenfunction corresponding to $U_1^{(1)}$.

It should be mentioned that the derivation of the complex Ginzburg–Landau equation is by no means trivial when the radial structures of the modes are taken into account. We should bear in mind that W_l is a differential operator, so that at any order and for each harmonic, a second-order complex ordinary differential equation has to be solved. This was done numerically using a standard Runge–Kutta method (Fehlberg 1985). The integrals in (30) were calculated in the same way. Specific results are presented in the next section.

4. Results

A set of parameters similar to those of Bekki (1981) has been used to obtain characteristic values for a low-pressure argon discharge: $\gamma = -0.5$, $\zeta = 1.0$, $\kappa = 1.0$, $D = b_i = 0.026$, $z_n = 0.751$, $z_{nn} = -1.0$, $z_{nnn} = 0$, $z_T = 8.5$, $z_{TT} = 56$, $z_{TTT} = 242$, $z_{nT} = z_{nTT} = z_{nnt} = 0$, $h_T = 3.5$, $h_{TT} = -5.5$ and $h_{TTT} = 11$. These dimensionless values correspond to a plasma density $n_0(0) = 2.7 \times 10^{12}\mathrm{cm}^{-3}$ and a pressure $p_0 = 0.9\,\mathrm{torr}$ (reduced to 0°C). The parallel electric field is $E_0 = 0.36$ V cm^{-1}, the temperature $T = 1.3$ eV, the discharge current $I = 2.5$ A, the ionization rate $Z = 5.0 \times 10^3$ s^{-1} and the electron mobility $b_e = 5.0 \times 10^4$ cm^2 V^{-1} s^{-1}. The critical parameters (in dimensionless form) are $k_{\mathrm{crit}} = 3.67$, $\omega_{\mathrm{crit}} = 1.85$, $\omega'(k_{\mathrm{crit}}) = -0.33$ and $\omega''(k_{\mathrm{crit}}) = 0.109 - 0.205i$. Note that these values have been calculated from the formulae taking the radial structure into account. The evaluation of the coefficients (29) and (30) yields $P_2 = 0.054 - 0.103i$ and $Q = 7.77 + 0.012i$.

In order to visualize the main effects, we simulated the dynamics of the wave of stratification numerically. We used a standard operator splitting scheme: the linear and nonlinear parts were calculated separately. Neglecting the imaginary parts of P_2 and Q (i.e. writing $P_2 \equiv P_{2R}$ and $Q \equiv Q_R$), (28) becomes a cubic nonlinear Schrödinger equation, which possesses the well-known solitons as stationary solutions. Starting with such a soliton in (28), we found the influence of the additional damping terms. Figure 3 shows the development of an initial soliton solution $(2/Q_R)^{1/2}\eta\,\mathrm{sech}(\eta z/{P_{2R}}^{1/2})$ with $\eta = 0.2$. For $\phi(\tau, \xi) = u(t = \tau, z = \xi + \lambda\tau)$, we have

$$iu_t + i\lambda u_z + P_2 u_{zz} + Q|u|^2 u = 0. \tag{31}$$

Here λ is, according to (27), the group velocity ω' in the laboratory frame. It is observed that the pulse is strongly damped while moving along the discharge tube. There are two reasons for the damping. The first originates from the linear dispersion relation near the critical point ($\mathrm{Im}(P_2) \neq 0$). All axial modes, except the critical one, are linearly damped. In addition, we have a nonlinear damping ($\mathrm{Im}(Q) \neq 0$). Let us briefly discuss the origins of the two damping terms. The linear one ($\mathrm{Im}(P_2) \neq 0$) is the familiar one, since it follows from the linear dispersion

https://doi.org/10.1017/S0022377898006801 Published online by Cambridge University Press

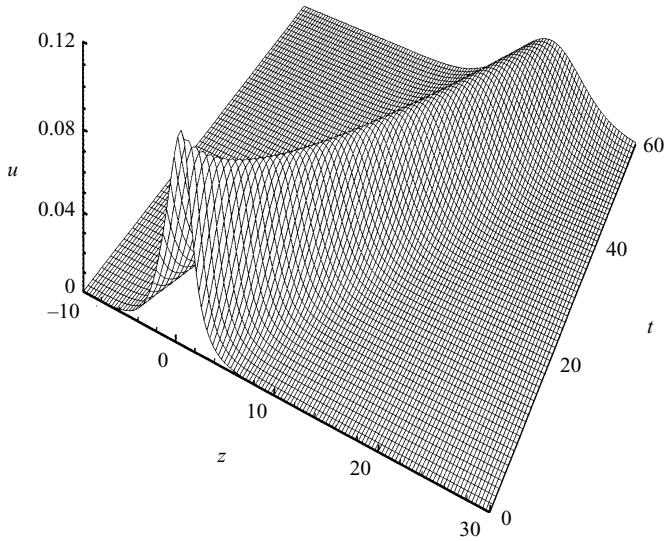


Figure 3. Development of an initial distribution $u(z, t = 0)$ (in the form of a so-called Schrödinger soliton) in time t according to the complex Ginzburg–Landau equation. Damping and dispersive broadening can be recognized.

relation. The linear damping is of the order of magnitude of the collisional damping rate of the mode with the central wavelength. The nonlinear damping ($\mathrm{Im}(Q) \neq 0$) occurs via mode coupling. The central mode couples nonlinearly to some (linearly) strongly damped waves. Owing to this process, an effective (additional) damping of the central mode appears. The nonlinear damping is thus proportional to the (square) of the amplitudes and the (linear) damping of non-central modes. These are two competing effects, since for weak nonlinearities the amplitudes are (still) small and the damping rates of the non-central modes are (relatively) strong. The nonlinear damping depends on the mode-coupling process, and the values of the corresponding integrals depend on the (radial) mode structures. Thus it is expected that (i) for infinitesimally small amplitudes the nonlinear damping vanishes and (ii) only the present calculation with the correct radial mode structures leads to the correct coupling coefficients. The latter can be significantly smaller than those calculated with the same (radial) mode structures for all waves. The effect of the nonlinear damping can be determined by comparing solutions for $\mathrm{Im}(Q) = 0$ with those for $\mathrm{Im}(Q) \neq 0$. In general, on the basis of an exact theory with radial structure of the ionization wave, the nonlinear damping turns out to be weak. This means that the total damping is dominated by the dispersive term in the complex Ginzburg–Landau equation (28). The situation is different when the radial structure of the ionization wave is not taken into account. In order to have an exact marginal state in that situation, we choose $z_n = 0.681$. The other dimensionless parameters of the critical point then follow as $k_{\mathrm{crit}} = 3.64$, $\omega_{\mathrm{crit}} = 1.78$, $\omega'(k_{\mathrm{crit}}) = -0.34$ and $\omega''(k_{\mathrm{crit}}) = 0.102 - 0.204i$. This leads to $P_2 = 0.051 - 0.102i$ and $Q = 7.51 + 1.57i$. Comparing with the previous case, we find quite good agreement for P_2. This shows that the use of the simplified model (without radial structure) is not too bad when calculating linear effects. The reason for this agreement lies in the coincidence of the radial structure of the homogeneous column with the radial structure of the ionization wave. This behaviour was confirmed experimentally by Ohe *et al.* (1991),

https://doi.org/10.1017/S0022377898006801 Published online by Cambridge University Press

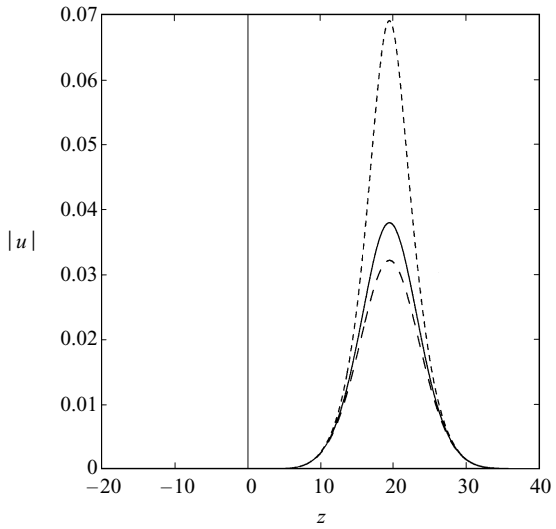


Figure 4. Absolute value of a solution of the complex Ginzburg–Landau equation over z at a fixed time $t = 60$. The solid line shows the exact solution with almost-vanishing nonlinear damping ($\mathrm{Im}(Q) \approx 0.01$), the long-dashed line correponds to a solution with coefficients calculated when the radial structure is neglected ($\mathrm{Im}(Q) \approx 0.16$). Finally, the short-dashed line is obtained when the dispersive damping is changed to growth ($\mathrm{Im}(Q) \approx -2.5$). In all cases $P_2 \approx 0.05 - 0.1i$.

and it supports our results. However, there is a large difference in the nonlinear coefficients Q. The imaginary part $\mathrm{Im}(Q)$ is much greater in the simplified model ($\mathrm{Im}(Q) \approx 1.6$) than in the more exact calculation considering the radial structure ($\mathrm{Im}(Q) \approx 0.01$).

The physical effect introduced by a positive $\mathrm{Im}(Q)$ is to damp the wave of stratification. Thus a smaller damping means larger amplitudes of the saturated wave. The next question is the relative importance of the nonlinear damping compared with the linear one. Let us consider (see Figs 3 and 4) an initial envelope with maximum amplitude ≈ 0.1. In Fig. 4 the solutions are then shown at a later time ($t = 60$) for three different situations. First (solid line for $\mathrm{Im}(Q) \approx 0.01$) the solution is presented for the case when the full radial structure is taken into account. As expected, a damping has occurred The damping is, however, less than in the corresponding simpler model (long-dashed line for $\mathrm{Im}(Q) \approx 0.16$) where the radial structure is ignored. Although the difference in the nonlinear damping rates is enormous, the final solutions are similar. That means that the total damping is dominated by the linear terms ($\mathrm{Im}(P_2) \approx -0.1$), at least in the chosen parameter regime. We have demonstrated this in Fig. 4 by the third curve (short-dashed line for $\mathrm{Im}(Q) \approx -2.5$). Although we have switched (artificially) from nonlinear damping ($\mathrm{Im}(Q) > 0$) to nonlinear growth ($\mathrm{Im}(Q) \approx -2.5 < 0$), the total damping survives owing to the linear effects ($\mathrm{Im}(P_2) \approx -0.1$).

Obviously, the effect of nonlinear damping will become more important for larger amplitudes. Our calculations, however, show that in realistic systems this effect will be significant only at very large amplitudes, being much larger than any estimate based on a simple model neglecting the radial structure. In addition, the present calculations show that $\mathrm{Im}(P_2)$ should not be neglected in the models for nonlinear waves of stratification. It is clear from a Fourier transformation of the linear

https://doi.org/10.1017/S0022377898006801 Published online by Cambridge University Press

part of (28) that $\mathrm{Im}(P_2)$ introduces a frequency-dependent damping of the initial distribution, as is seen in our numerical simulations.

5. Summary

In order to find out whether the commonly used one-dimensional models for the wave of stratification are applicable, we have developed a model that takes care of the radial structure. We have investigated the marginally stable situation and taken into account the dependence of the ionization rate on the radial density distribution.

In the linear regime, a variety of modes exist. We have picked out the one that is least damped. This mode has approximately the same radial structure as the positive column itself. All other modes oscillate in the radial direction, and diffusion leads to their damping. The radial distribution of the wave of stratification is very close to the radial variation of the homogeneous positive column.

It has been shown that, in principle, two coefficients determine the dynamics of the wave of stratification. These coefficients of the nonlinear Ginzburg–Landau equation (28) have been calculated numerically. Both coefficients are complex. The imaginary part of the dispersion coefficient (P_2) – considered here for the first time in the nonlinear wave dynamics – introduces a frequency-dependent damping. It turns out that it dominates the evolution of the wave packet. The imaginary part of the dispersion coefficient (P_2) is larger than the real part. On the other hand, the real part of the nonlinear coefficient (Q) dominates the imaginary part. The latter causes only a weak nonlinear damping when the radial structure is taken into account consistently. When simulating the complex Ginzburg–Landau equation (for a Schrödinger soliton as initial condition), we have demonstrated the importance of dispersive damping for the evolution of the wave of stratification.

Acknowledgements

This work was performed within in the Sonderforschungsbereich 191 'Physikalische Grundlagen der Niedertemperaturplasmaphysik'. It is part of the PhD thesis of one of us (M.R., Klauder (1996)).

References

Bekki, N. 1981 Nonlinear modulation of ionization waves. *J. Phys. Soc. Japan* **50**, 659–667.

Fehlberg, E. 1985 Some old and new Runge–Kutta formulas with stepsize control and their error coefficients. *Computing* **34**, 265–270.

Hasegawa, A. 1990 *Solitons in Optical Fibers.* Springer-Verlag, Berlin.

Klauder, M. 1996 Nichtlineare Ionisationswellen mit radialer Struktur. PhD thesis, Heinrich-Heine-Universität Düsseldorf.

Landa, P. S. 1996 *Nonlinear Oscillations and Waves in Dynamical Systems*. Kluwer, Dordrecht.

Landa, P. S., Miskinova, N. A. and Ponomarev, Y. V. 1980 Ionization waves in low-temperature plasmas. *Soviet Phys. Usp.* **23**, 813–834.

Mitchner, M. and Kruger, C. H. 1973 *Partially Ionized Gases.* Wiley, New York

Nedospasov, A. V. 1968 Striations. *Soviet Phys. Usp.* **11**, 174–187.

Newell, A. C. and Whitehead, J. A. 1969 Finite bandwidth, finite amplitude convection. *J. Fluid Mech.* **38**, 279–303.

Ohe, K., Naito, A., Kimura, T. and Iwama, N. 1991 Three-dimensional structure of finite-amplitude ionization wave packets excited in the positive columns. *Phys. Fluids* B **3**, 3302–3311.

https://doi.org/10.1017/S0022377898006801 Published online by Cambridge University Press

Oleson, N. L. and Cooper, A. W. 1968 Moving striations. *Adv. Electron. Phys.* **24**, 155–278.

Papoular, R. 1965 *Electrical Phenomena in Gases*. Iliffe, London.

Pekarek, L. 1968 Ionization waves (striations) in a discharge plasma. *Soviet Phys. Usp.* **11**, 188–208.

Pfau, S., Rutscher, A. and Wojaczek, K. 1969 Das Ähnlichkeitsgesetz für quasineutrale anisotherme Entladungssäulen. *Beitr. Plasma Phys.* **9**, 333–358.

Shkarofsky, I. P., Johnston, T. W. and Bachynski, M. P. 1966 *The Particle Kinetics of Plasmas*. Addison-Wesley, Reading, MA.

Twomey, D. and Franklin, R. N. 1974 Ion waves and ionization waves in a plasma of finite radius. *J. Phys.* **D7**, 1963–1974.

Wojaczek, K. 1962 Zur Bestimmung laufender Schichten kleiner Amplitude in Niederdruckentladungen. *Beitr. Plasma Phys.* **2**, 1–12.

Yoshimoto, H. and Yamashita, Y. 1967 Dispersion relation of moving striations. *J. Phys. Soc. Japan* **22**, 1087–1093.

https://doi.org/10.1017/S0022377898006801 Published online by Cambridge University Press